WILEY InterScience® DISCOVER SOMETHING GREAT

PROTEINS STRUCTURE ■ FUNCTION ■ BIOINFORMATICS

Dynamics of heteropentameric nicotinic acetylcholine receptor: Implications of the gating mechanism

Agnieszka Szarecka,[1] Yan Xu,[1,2] and Pei Tang[1,2,3]*

[1] Departments of Anesthesiology, University of Pittsburgh School of Medicine, Pittsburgh, Pennsylvania 15261

[2] Departments of Pharmacology, University of Pittsburgh School of Medicine, Pittsburgh, Pennsylvania 15261

[3] Departments of Computational Biology, University of Pittsburgh School of Medicine, Pittsburgh, Pennsylvania 15261

ABSTRACT

The dynamics characteristics of the currently available structure of* Torpedo *nicotinic acetylcholine receptor (nAChR), including the extracellular, transmembrane, and intracellular domains (ICDs), were analyzed using the Gaussian Network Model (GNM) and Anisotropic Network Model (ANM). We found that a symmetric quaternary twist motion, reported previously in the literature in a homopentameric receptor (Cheng et al. J Mol Biol 2006;355:310–324; Taly et al. Biophys J 2005;88:3954–3965), occurred also in the heteropentameric Torpedo nAChR. We believe, however, that the symmetric twist alone is not sufficient to explain a large body of experimental data indicating asymmetry and subunit nonequivalence during gating. Here we report our results supporting the hypothesis that a combination of symmetric and asymmetric motions opens the gate. We show that the asymmetric motion involves tilting of the TM2 helices. Furthermore, our study reveals three additional aspects of channel dynamics: (1) loop A serves as an allosteric mediator between the ligand binding loops and those at the domain interface, particularly the linker between TM2 and TM3; (2) the ICD can modulate the pore dynamics and thus should not be neglected in gating studies; and (3) the F loops, which are peculiarly longer and poorly-conserved in non-α-subunits, have important dynamical implications.

Proteins 2007; 68:948–960.
© 2007 Wiley-Liss, Inc.

***Key words:* nicotinic acetylcholine receptor; Cys-loop receptors; gating; normal modes; quaternary twist; Gaussian network model (GNM); anisotropic network model (ANM).**

INTRODUCTION

The nicotinic acetylcholine receptor (nAChR) is a member of the Cys-loop superfamily, which also includes γ-aminobutyric acid type A ($GABA_A$), glycine (Gly), and serotonin ($5\text{-}HT_3$) receptors.[3,4] These receptors switch between ion-permeable and -impermeable conformations via neurotransmitter binding and unbinding to facilitate fast synaptic transmission. Malfunction of these receptors is associated with various diseases.[5] All Cys-loop receptors are composed of five homologous subunits that are arranged pseudosymmetrically around a central ion channel. Each subunit consists of an extracellular N-terminal ligand-binding domain (LBD), four transmembrane domains (TMDs, TM1–TM4), an intracellular domain (ICD), and a short C-terminus. Structurally, nAChR is better characterized than the other members of the superfamily. Because the acetylcholine binding protein (AChBP) shares considerable sequence identity with the LBD of nAChR (nAChR-LBD) and also because its relevance to the Cys-loop receptor family has been confirmed by its pharmacological characteristics,[6–8] the high-resolution crystallographic structures of AChBP[9–12] have yielded important insights into the activated or desensitized nAChR-LBD. A recent atomic scale model of the *Torpedo* nAChR at 4-Å resolution[13,14] provides further structural information on the receptor in the resting state. In the *Torpedo* nAChR, which has subunit stoichiometry of $\alpha_2\beta\delta\gamma$, the ligand binding sites are located at the αγ and αδ interfaces in LBD, involving primarily loops A, B, and C from the α-subunit and the residues from the so-called complementary side of the partner γ- and δ-subunits. Despite this large body of experimental data, the exact nature of the linkage between ligand binding and channel gating remains elusive. Several possible "communicators" between LBD and TMD have been proposed, including the loop between TM2 and TM3 in the TMD[15–17] and the loops between β1 and β2, β4 and β5 (loop A), and CYS in the extracellular domain.[18,19] These insights from structural models have recently inspired new designs of experiments[20,21] that can further advance our understanding of not only nAChR but also other receptors in the superfamily.

The Supplementary Material referred to in this article can be found online at http://www.interscience.wiley.com/jpages/0887-3585/suppmat/

Grant sponsor: National Institutes of Health; Grant numbers: R01GM066358, R01GM056257, R37GM049202.

*Correspondence to: Pei Tang, Ph.D., University of Pittsburgh School of Medicine, Biomedical Science Tower 3, Room 2049, 3501 Fifth Avenue, Pittsburgh, PA 15260. E-mail: tangp@anes.upmc.edu

Received 9 November 2006; Revised 30 January 2007; Accepted 9 February 2007

Published online 1 June 2007 in Wiley InterScience (www.interscience.wiley.com). DOI: 10.1002/prot.21462

© 2007 WILEY-LISS, INC.

Along with the progress made in acquiring structural information, a significant amount of effort has also been devoted to obtaining a comprehensive and coherent picture of nAChR dynamics in association with its function. Charge reversal and charge neutralization mutations at the interface of LBD and TMD have led to a unified view of the role of electrostatic interactions in modulating the gating of Cys-loop receptors.[22] On the basis of combined electrophysiology and mutagenesis studies, it is hypothesized that the conformational change occurs "in a wave-like manner" along the long axis of the channel[23]; only a few discrete "blocks" are coupled with the "low-to-high" affinity change at the ligand-binding sites before the opening of the channel.[19] The cryoelectron microscopy data collected on the *Torpedo* nAChRs in the presence or absence of acetylcholine[24] revealed an asymmetric motion within the LBD. Several other studies[25–27] on muscle-type nAChRs provided additional evidence of asymmetry in the quaternary movement during gating.

The exact location and nature of the gate are also uncertain. Some experimental data[28,29] support the notion that the gate locates near the intracellular end of the pore. Other experimental[13] and computational[30,31] data suggest a hydrophobic nature of restricting ion flow rather than physical narrowing of the pore diameter and locate the gate in the mid-section of TM2 helices.

Computational studies have also yielded a wealth of information about the receptor's dynamics, ion and water permeation, possible gating motions, and channel function.[31–37] A substantial degree of asymmetry in the subunit motion and the distinctive behavior of two nonadjacent subunits of the homopentameric α7 nAChR were observed in molecular dynamic simulations,[35,38,39] although these were rather short simulations and may have suffered from insufficient sampling. In contrast, two variants of normal mode analysis (NMA) on the same receptor[1,2] indicated a highly symmetric movement of the subunits in the lowest frequency mode, i.e. a concerted rotation of LBD and TMD with respect to each other. This motion was implicated in gating, and a pore widening was also documented. In addition, similar type of twisting motion was recently reported in a study of a set of potassium channels.[40] However, most of the Cys-loop receptors are heteropentameric with asymmetric interfaces and nonequivalent binding sites. It is difficult to envision a link between the asymmetric gating stimulus and a symmetric, highly collective rotational motion. Other findings that indicate asymmetric changes during gating cannot be explained by the symmetric rotation only. Another potential problem with recently proposed computational models is the lack of ICD, the importance of which has been experimentally confirmed and reviewed recently.[41] The ICD not only links the channel with cytoplasmic proteins but also directly affects channel kinetics,[42,43] ion flow restriction,[44] and desensitization.[45]

In the present study, we investigated the dynamics of nAChR with two coarse-grained elastic network models: Gaussian network model (GNM) and anisotropic network model (ANM).[46–48] Both have been shown to be powerful and robust tools for characterizing the low-frequency collective motions of large biomolecules and assemblies.[40,49–54] We are primarily interested in identifying and characterizing the vibrational modes corresponding to motions that may gate the structurally asymmetric channel. In this context, we identify asymmetric motions that are necessary—perhaps in combination with the symmetric twist—to change the pore size and shape in our model.

METHODS

Starting structure

The starting structural model was the ligand-free heteropentameric *Torpedo* nAChR from the cryoelectron microscopy data (pdb code 2BG9)[14] and included the intracellular (cytoplasmic) domain in addition to the TMD and extracellular LBD. Figure 1 displays the details of the receptor structure along with the naming and the locations of the crucial segments discussed in this paper.

Elastic network models

GNM and ANM[46,55,56] are derived from the elastic networks theory and assume that a protein in its folded state can be represented by a three-dimensional elastic network whose nodes fluctuate with Gaussian distribution in the uniform harmonic potential of their close neighbors. Protein model is coarse-grained by adopting one atom (usually C^{α}) per residue. Residues are connected to their neighbors, irrespective of bonded and nonbonded, by springs of a uniform force constant, γ, the value of which is adjustable to match the normalized distribution of the computational to the experimental B factors. A list of neighbors is determined by interaction cutoff radius R_C. The mean square fluctuations for each residue can be calculated as contributions from separate vibrational modes or from any subset of modes in GNM and ANM. GNM yields squared fluctuations without any information about the directionality of the motion, whereas ANM provides *X*, *Y*, *Z* components of the fluctuations, allowing for the interpretation of the motion in relation to the biological function. Particularly, the slowest modes of GNM and ANM represent the large-amplitude, lowest-frequency collective motions that are usually of functional importance.[49] This functional relevance stems from the fact that, even though NMA yields vibrational characteristic of the system near its native equilibrium state, the resultant eigenvectors still correlate very well with directions of conformational transitions between different equilibrium states.[57] Proteins use their

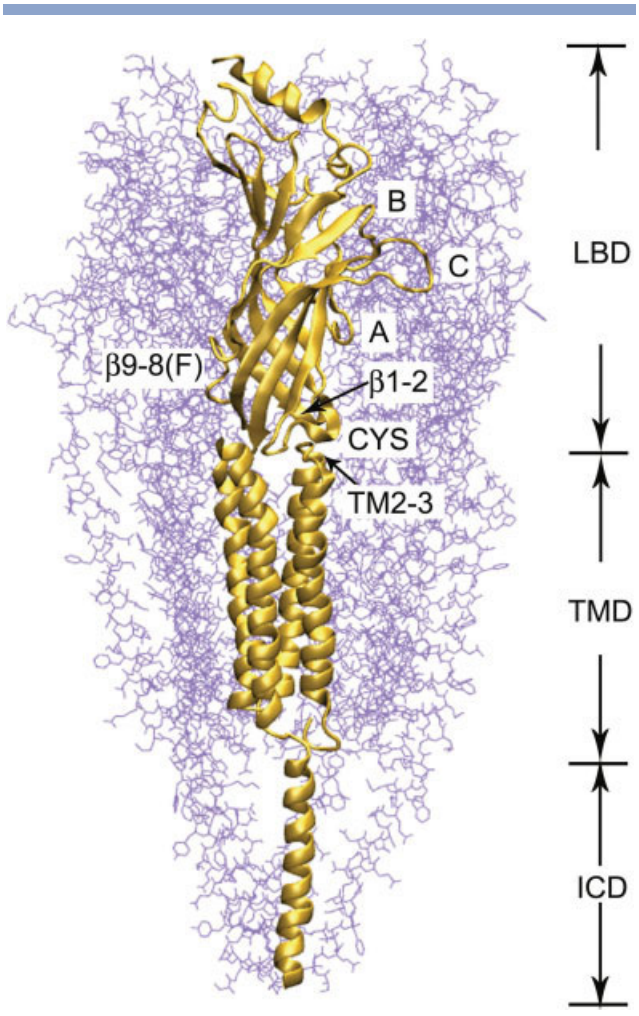

Figure 1

The α-subunit of the Torpedo *nAChR. Important loops in the ligand binding and transmembrane domains discussed in this paper are labeled. LBD: ligand-binding domain; TMD: transmembrane domain; ICD: intracellular domain.*

native state dynamics to *initiate* the transition hence the observed directional correlations.[57,58]

A detailed description of the theory can be found in the literature.[46,55] A brief outline of the theory and essential equations can be found in the supplemental material accompanying this paper.

All calculations were performed using the programs based on GNM/ANM codes obtained from http://ribosome.bb.iastate.edu/software.html on a Dell Precision 530 workstation equipped with dual 1.8-GHz Xeon processors. Online servers, performing GNM and ANM calculations (http://ignm.ccbb.pitt.edu/GNM_Online_Calculation.htm[49,59] and http://ignmtest.ccbb.pitt.edu/cgi-bin/anm/anm1.cgi) as well as another elastic network-based calculation server (http://www.igs.cnrs-mrs.fr/elnemo/[60–62]), were also used. Determination of the optimal cutoff radii for GNM/ANM calculations, with the aid of acetylcholine binding protein (AChBP, pdb 1I9B),[9] is described in detail in the supplemental materials.

Correlations were calculated between squared fluctuations yielded by GNM and ANM modes to ascertain correspondence between both methods. However, it should be recognized that there is no one-to-one correspondence between the GNM and ANM modes and the amplitudinal correlation coefficients are expected to be moderate. In our case, the correlation coefficients are in the range of 0.7–0.8 and 0.4–0.6 for the twist and asymmetric modes, respectively.

Hypothetical open-state conformation

Our open-pore models of the receptor were obtained using the eigenvectors corresponding to three types of receptor motions. The C^{α} coordinates were obtained in a similar fashion to that described previously,[40] using

$$[\mathbf{R}(\pm)]_k = \mathbf{R}^0 \pm s_k \lambda_k^{-1/2} \mu_k \qquad (1)$$

where $\mathbf{R}$ and $\mathbf{R}^0$ are the instantaneous and original $3N$-dimensional vectors (N being the number of residues) of C^{α} coordinates, respectively, λ_k and μ_k are the eigenvalue and eigenvector, respectively, of the kth mode. The "amplification" parameter s_k was set to 100.

We have also attempted at obtaining a hypothetical open-state all-atom structure of the receptor using only the eigenvector corresponding to the symmetrical twist motion. The procedure involved multiple cycles of small C^{α} atom displacements along the eigenvector in two opposite directions, generating both clockwise and counterclockwise pore-opening conformations. The resulting structures in each cycle underwent constrained and unconstrained energy minimizations using the program NAMD[63] to relax the backbone and side chains around the new positions of C^{α}. Pore radii were estimated using programs Hole[64] and VMD.[65]

Modeling the missing F loops

Unresolved residues in the structure of the extracellular domains of non-α-subunits, namely, residues 165–173, 163–177, and 165–171 in the β8-9 (F) loop of subunits β, δ, and γ, respectively, were modeled using the MODELLER program.[66,67] The stereochemical quality of the resultant loop conformations was subsequently evaluated with PROCHECK.[68] A large number of loop conformations have been generated and several lowest energy structures have been tested for their impact on the receptor's dynamics.

RESULTS AND DISCUSSION

In the following sections we present our data in support of the hypothesis that gating motion in the TMD of

DOI 10.1002/prot

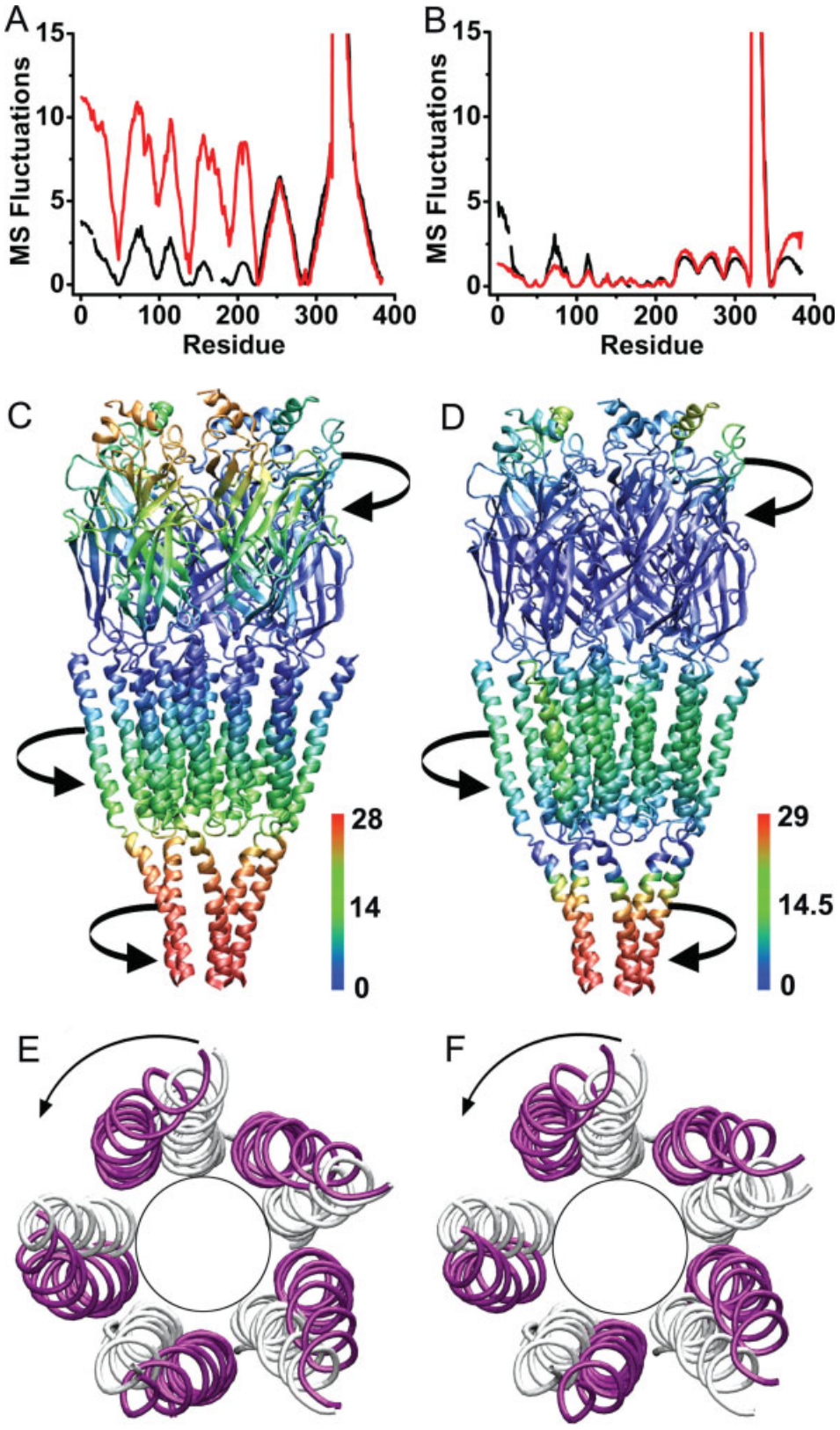

Figure 2

*Quasisymmetric twisting motion of the heteropentameric muscle-type nACh receptor. GNM mean square (MS) fluctuations [$\times 10^{-3}$] of mode 1 (**A**) and mode 4 (**B**), corresponding to type I and type II twisting motion, respectively, are plotted as a function of residue numbers for the α- (α^{γ}, black) and non-α- (δ, red) subunits. Notice the difference in type I motion of LBDs (residues 1–225) between α and non-α-subunits. The fluctuation values are color-coded onto the nAChR structure (red: high; green: moderate; blue: low) for type I (C) and type II (D) motions. The black arrows show the phases of the twisting directions from the correlated ANM modes. The TM2 domains from the models of open-pore structures (magenta) calculated from ANM eigenvectors and eigenvalues (see Methods) are compared with the starting close-pore structure (gray) for type I (E) and type II (F) twists. The black circles are drawn to guide the eyes only. Notice the widening of the pore as a result of the twists.*

the asymmetric, heteropentameric receptors is not purely a quasisymmetric rotation (called a quaternary twist) as suggested in recent articles[1,2] but requires a contribution from an asymmetric tilting.

Further, we discuss three additional aspects related to gating in heteropentameric receptors, namely (i) cross-correlation maps that reveal dynamical connections within and between subunits, (ii) impact of ICD on the receptor, and (iii) role of F loops in non-α-subunits.

Symmetric twist motion

Our GNM and ANM analyses of the heteropentameric *Torpedo* nAChR (including LBD, TMD, and ICD) revealed two types of a quasisymmetric twisting motions (Fig. 2) among the slowest modes. Type I motion consists of LBD twisting in the opposite direction from TMD and ICD while the latter two move as a single coherent unit [see Fig. 2(C)]. In type II motion, LBD, TMD, and ICD twist in the opposite directions relative to their immediate neighbors [see Fig. 2(D)]. The GNM mean-squared fluctuations (MSFs) from modes 1 and 4 are depicted in Figure 2(A,B), respectively. To visualize the MSF distribution, the fluctuation values are color-coded onto the receptor structures in Figure 2(C,D), along with the directions of the concerted twists revealed by the ANM analyses. Even in these quasisymmetric twisting modes, the fluctuation distributions are less symmetric in LBD than in TMD and ICD. This is particularly so in type I motion [mode 1, Fig. 2(A,C)] where subunits β and δ fluctuate more intensely than subunits α–γ–α. Also noticeable in type I motion is that the LBD–TMD interface and the top half of the TMD are rigid, while the bottom half of the pore domain and the intracellular helices are mobile. This type I twist is analogous to the previously reported quaternary twist found in the neuronal $(\alpha_7)_5$ nAChR using two different variants of NMA.[1,2] The hinge point of this motion lies in the LBD–TMD interface. The type II motion is mostly symmetrical [Fig. 2(B,D)] and exhibits very low flexibility in the LBD and at the interfaces between LBD and TMD and between TMD and ICD. The ICD is again very mobile in type II motion. The transmembrane pore helices are flexible, especially in their middle sections where a hydrophobic gate has been proposed.[30,31] Compared to type I, the type II twist [mode 4, Fig. 2(B,D)] represents decoupling of TMD and ICD, with additional hinge points at the TMD–ICD interface. Although the amplitudes of ICD motion might be exaggerated in both types due to incompleteness of the ICD structure, the nature of the motion relative to other domains is likely to be correctly captured by the GNM and ANM analysis.

It was suggested based on the NMA of the homopentameric neuronal $(\alpha_7)_5$ nAChR[1,2] that the symmetric twisting motion occurred as one of the lowest-frequency modes and caused significant pore widening. We have created models of the open-channel conformation using the ANM eigenvectors [Eq. (1)] and compared their TM2 (pore) helices with the close-channel structure. Figure 2(E,F) show the pore-lining segments in the conformations before and after the backbone displacement along the eigenvectors for type I (mode 1) and type II (mode 4) twists, respectively. The models show clearly that both types cause certain degrees of pore widening. This is particularly apparent in the C^{α} model displaying only the backbone pore dilation. However, when we attempted at building an all-atom model of the open channel by using the type I eigenvector on C^{α} followed by reconstruction of all other atomic positions, allowing for ∼3.5-Å backbone RMSD from the reference structure, we only achieved a 1.4-Å increase in pore diameter. Although this increase does not appear enough for an open channel based on permeability studies,[69] other investigators have suggested that relatively minor displacements in the gate area can trigger the functional transition of the pore from close to open.[31,70] We have also compared the two structures resulting from displacements in the opposite directions of the TMD twist motion. Although the directional preference is not significant in terms of changes in pore size, a counterclockwise collective motion of LBD (i.e., a clockwise motion of TMD as viewed from the extracellular domain) can produce a certain degree of closeness between the C loop and the subunit interface. The tendency to close the C loop is more favorable for agonist binding than that to open the C loop by a clockwise LBD twist motion.

A rigid TMD–ICD interface in type II twist may have interesting implications, as this region along with the entire ICD is thought to form a selectivity filter.[14] It was proposed previously that the location of the gate might be at the cytoplasmic end of the pore[29] and that there could be two dynamically separate gates for the resting and desensitized receptors.[71] Although the incompleteness of the ICD in the currently available structure precludes a definitive conclusion to be drawn about the dynamics of this region, our observation that two different types of symmetric twist motion exist to couple ICD and TMD helices nevertheless suggests the necessity of including ICD in the assessment of the functional dynamics of nAChR.

In summary, two types of symmetric twist motion are present in the heteropentameric nAChR containing the ICD. The twist motions are shown to increase the pore diameter and thus likely to contribute to channel gating.

Asymmetric tilting motion

Although the quaternary twists are reasonable motion candidates for gating because they involve the long-speculated helical rotations[13] and lead to pore dilation, the question remains as to whether the symmetric twists alone are sufficient to cause gating.

DOI 10.1002/prot

First, it is difficult to reconcile the quasisymmetric LDB dynamics in the symmetric twist motion with the fact that the gating in the *Torpedo* nAChR is triggered asymmetrically by the motion of the α-subunits in LBD, while the non-α-subunits only provide a framework for this motion.[14,24] Furthermore, the quaternary twist motion is highly symmetric in the pore region and involves all subunits equally. This is in contradiction to some experimental data indicating a strongly nonequivalent contribution of different subunits to gating.[25,27]

Second, the neurotransmitter binding pocket shows a "passive" dynamical characteristic in the twist motion. The loops embracing the binding pocket, including loops A, B, and C on the primary side of the α-subunits and the F loop on the complementary side of the non-α-subunits, move collectively with their subunits. Although a counterclockwise LBD twist brings the C loop closer to the subunit interface than a clockwise twist, there is no sign of the independent C-loop swinging motion that could bring the C loop close enough to the subunit interface to facilitate ligand binding as suggested by the X-ray studies of the acetylcholine binding protein, a well-established model for the LBD of the acetylcholine and other Cys-loop receptors. Changes in the C-loop conformation have been reported as major differences amongst the apo, agonist-bound, and antagonist-bound forms of AChBP.[72]

Finally, there is also evidence for a plausible scenario where sequential rather than concerted movement takes place during gating.[23,26] Thus, it is possible that a chain of events involving a set of conformational changes contributes to the channel opening.

Among the low-frequency GNM modes, we identified two additional types of motion—referred here as type III and type IV—that displayed some of the aforementioned characteristics, as shown in Fig. 3, and thus can explain the experimental findings that cannot be explained by the symmetric twists. Both type III and type IV motions are asymmetric and exhibit significantly more mobility in the α than the non-α-subunits. This distinction in flexibility between the α- versus non-α-subunits is reminiscent of a model proposed by Unwin,[14] in which α-subunits as the gating triggers undergo major conformation changes. Type III and type IV are distinguishable from each other by the fluctuation patterns in the α-subunits. In type III [Fig. 3(A)], the LBDs of the α-subunits are highly mobile. The high flexibility regions include the top α-helix, the β2–3 and β5′–6 loops, and the C loop at the ligand binding site. Flexibility remains moderate at the LBD–TMD interface (including loops CYS, β1–2, and TM2–3) and gradually decreases downward to the pore. In contrast, the type IV motion shows an interesting shift in the regions of flexibility: the mobility is decreased in the binding loops and the inner sheet but increased at the LBD–TMD interface, the pore-lining TM2 helices, and the ICD helices. The α-subunit dominance in fluctuation also becomes less pronounced in the type IV asymmetric motion due to an increasing mobility in other subunits, particularly the δ-subunit in the pore region. The marked increase in fluctuations of other TM helices is in line with the experimental data showing the mutual rearrangements and influence of all TM helices on gating.[4]

It is worth noting that type III and type IV fluctuation patterns revealed by GNM may represent the intrinsic modes of motion for potential conformational changes associated with ligand binding and subsequent signal propagation down to the pore region, assuming that the sequential wave-like rather than concerted mechanism governs the channel gating. It is thus of great importance to identify ANM modes corresponding to these two types of asymmetric GNM fluctuations. We determined the correlations between the MSF patterns of the GNM results and those constructed by summing the squares of the directional ANM fluctuations. We found that type III and type IV GNM fluctuations have fairly strong correlations with ANM modes 4, 5, and 13, with correlation coefficients ranging from 0.4 to 0.6. Additionally, type IV also correlates with ANM mode 11. ANM modes 4 and 5 are asymmetric bending and swinging with α–β–δ–α–γ subunits moving in an alternating in-and-out pattern with respect to the pore axis. The amplitude of these two ANM modes is very pronounced in LBD and tapers toward the ICD helices. Modes 11 and 13 resemble a "breathing" movement of the channel, where the top of the LBD bends in and out radically relative to the pore axis, triggering a propagation of displacement from LBD to the TMD and ICD. This motion produces expansion in the LBD–TMD interface, which in turn is coupled to the tilting motions of the TM2 helices and the bending of the ICD helices. In both cases, the TMD helices, particularly the pore-lining TM2 domains, exhibit a similar asymmetric tilting, as shown in Figure 3(C,D), causing deformation of channel passage in a motion-dependent manner. The pore shape changes considerably as a result. Although pore widening in asymmetric motion is not as pronounced as in the case of the symmetric twist, the helical tilting is sufficient to alter the hydrophobic profile of the channel lining. Previous reports already suggested that when the nature of a gate is hydrophobic instead of geometric occlusion, the required pore widening may be smaller than that commonly assumed.[31,70,73] In addition, asymmetry of the conformational changes in our model correlates with experimental findings on the unequal contributions from different subunits to the gating movement.[25,27]

More generally, our finding of important contributions from asymmetric modes to nAChR gating seems to suggest that the slowest normal modes of motion in the elastic network model do not necessarily correspond to the symmetry of the structure. This conclusion is compromised somewhat in our case because one could argue

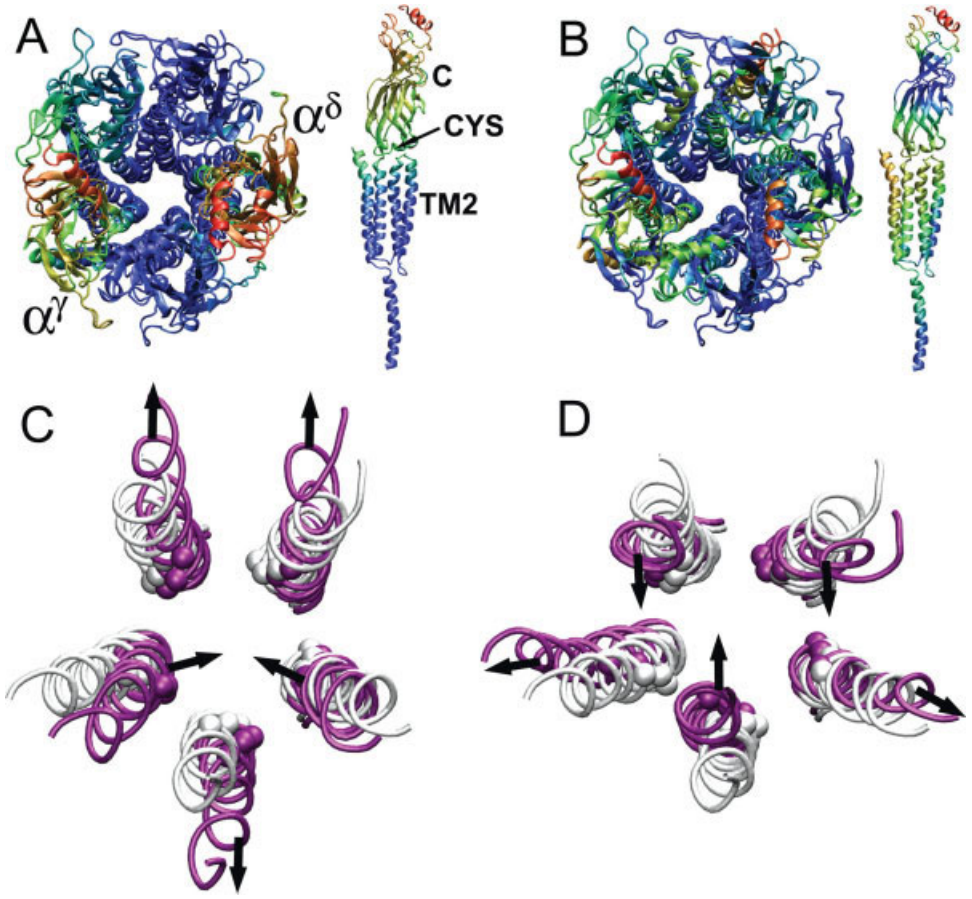

Figure 3

*Asymmetric motion of the heteropentameric nACh receptor. GNM mean square fluctuations, corresponding to type III (**A**) and type IV (**B**) asymmetric motions, are mapped onto the nAChR receptor structure (showing top view from the extracellular domain of the receptor and the side view of the α^{γ}-subunit). The fluctuation amplitude is color-coded as red for high, green for moderate, and blue for low. The side views show the high flexibility of the LBD in type III and of the transmembrane domain in type IV. TM2 pore profile changes due to displacements in two possible directions, calculated from the ANM modes corresponding to type IV asymmetric motion, are depicted in C and D before (gray) and after (magenta) the displacements. Notice the significant TM2 helix tilting and the dynamics dependence of the pore profile.*

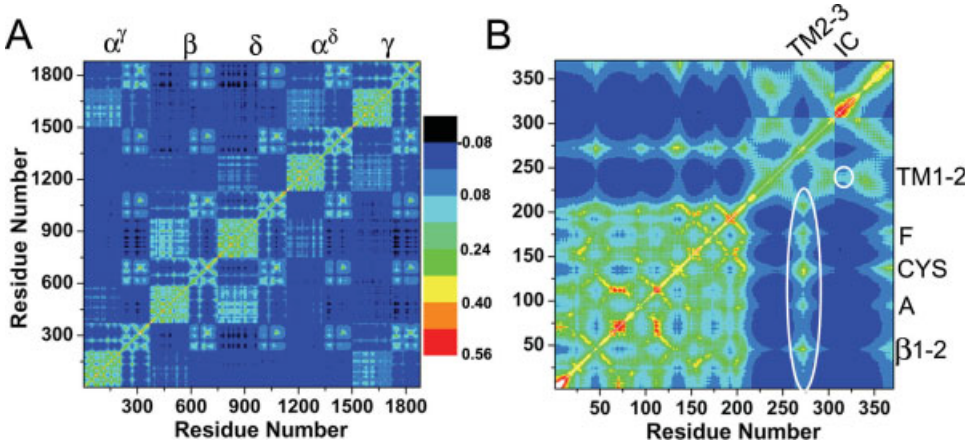

Figure 4

*Interresidue cross-correlations of all GNM modes for (**A**) the entire nAChR and (**B**) the α^{γ}-subunit. Strong long-range correlations exist among TMDs and intracellular helices from all five subunits, and between the LBD of the β- and δ-subunits. Within each subunit, the most important cross correlations between LBD and TMD are those of loop TM2-3 with loops A, F, CYS, and β1–2 (encircled within the white oval), which are likely to be the actuation points to communicate the events of ligand binding to channel gating. Positive correlations also exist between the intracellular helices and the TM1–2 loops of the same subunit as well as the preceding subunit (viewing counterclockwise from extracellular side).*

that the nonsymmetric motions might be the consequence of the heteropentameric assembly in the *Torpedo* nAChR. However, when we compared the ANM results of homopentamer AChBP and heteropentamer nAChR–LBD, we found similar types of motions in both cases, despite the fivefold symmetry in the structure of the former and the lack of perfect symmetry in the structure of the latter. Thus, it can be concluded that directional asymmetry is an intrinsic dynamics feature of this type of assemblies.

In summary, the intrinsic subdomain mobility is different for different subunits in the nAChR. The two α-subunits are significantly more mobile in the low-frequency asymmetric modes of motions. These motions seem to suggest the linkage between the events of ligand binding in LBD [Fig. 3(A)] and the propagation of the motion to TMD [Fig. 3(B)]. We propose that the superposition of the symmetric twist and the asymmetric tilting contributes to the gating of heteropentameric nAChR.

Other aspects of nAChR dynamics

Pathways from LBD to TMD

The preceding paragraphs were devoted to only one aspect of our understanding of channel gating, namely, the nature of the conformational change that can potentially transition the pore-lining helices into the ion-permeable shape. Another aspect of receptor function is how this change in TMD is effected by the ligand binding. Some insight into this question can be gained from the cross-correlation map that integrates all GNM or ANM modes and provides information about motional interdependencies between residues. Figure 4 depicts the cross-correlation map constructed from all GNM modes. Figure 4(A) presents a global map for the entire receptor (after appending residue numbers for five subunits), from which intersubunit correlations can be discerned. Figure 4B focuses on the intrasubunit cross-correlations using subunit α^{γ} as an example.

Figure 4(A) reveals several important features: (1) the intersubunit cross-correlations are positive in the TMDs; they are strong between adjacent subunits and relatively weak between remote subunits; (2) all of the ICD helices are strongly correlated; (3) the correlations between the TM2–3 loops in different subunits are weak and negligible; (4) a strong positive correlation of the LBDs is found between, and only between, subunits β and δ. It also shows that the intrasubunit patterns, while not identical, are very similar for all subunit types.

Among the intrasubunit cross-correlations, the most important ones are those that link the LBD and TMD and thus can act as the actuation points for signal propagating from the binding site to the gate. As shown in Figure 4(B), LBD is either noncorrelated or very weakly anticorrelated with TMD helices except for TM2–3, the loop linking TM2 and TM3. The TM2–3 loop correlates positively with several key loops in LBD, including loops β1–2, A, CYS, and F [see Fig. 4(B)]. The correlations between TM2–3 loop and β1–2 loop and between TM2–3 loop and CYS loop are particularly strong, suggesting that these loops may act as the contact points for LBD and TMD communication. The correlations between the TM2–3 loop and loop A (allosteric link) or loop F were not reported in a similar analysis performed previously on the homology model of the neuronal $(\alpha_7)_5$ receptor.[1] In addition, among the interfacial loops, it can be seen from Figure 4(B) that loop A also cross-correlates (although weakly) with (a) CYS and β1–2 loops, and (b) binding loop B that in turn is strongly coupled with loop C. Thus loop A is an important "mediator" between ligand binding segments and the domain interface. This finding is in agreement with previous experimental work.[18] There seems to be no correlation between loops A and F. Therefore, the gating through these two pathways may be independent.

In summary, in addition to the previously identified interactions of the TM2–3 loop with the CYS loop and the β1–2 loop, the important connection between the binding pocket and the interfacial loops resides at loop A. We also observed another potentially important link between loop F and loop TM2–3.

Dynamical impact of ICD helices

In the computational studies published so far, the ICD helices were neglected due to the lack of structural data or to the notion that solution to the gating problem lies solely in the TMD or LBD–TMD part of the receptor. It has become increasingly clear, however, that the role of ICD is much greater.[41] This was the reason why we used the "more complete" structure including the ICD in the present study. For comparison purpose, we also carried out parallel GNM and ANM analyses of the heteropentameric nAChR without the ICD. The global GNM mode corresponding to type I quaternary twist is depicted in Supplemental Figure 1S.

One aspect of the ICD influence on the pore dynamics was already discussed, i.e. the existence of two different types of symmetric quaternary twist. We believe that the dynamics at the interface between the TMD and ICD can be equally important as between LBD and TMD. The TMD–ICD interface is likely to be the location where gating, ion selection, and possibly the control of ion flow are coupled. A direct comparison of the twist mode obtained with and without the ICD [Figs. 2(C) and 1S] shows that neglecting ICD produces different dynamical patterns. Inclusion of the ICD modulates the fluctuation distribution affecting the entire receptor but most pronouncedly the TMD.

Another important aspect of the ICD influence on channel dynamics is the positive correlation between ICD

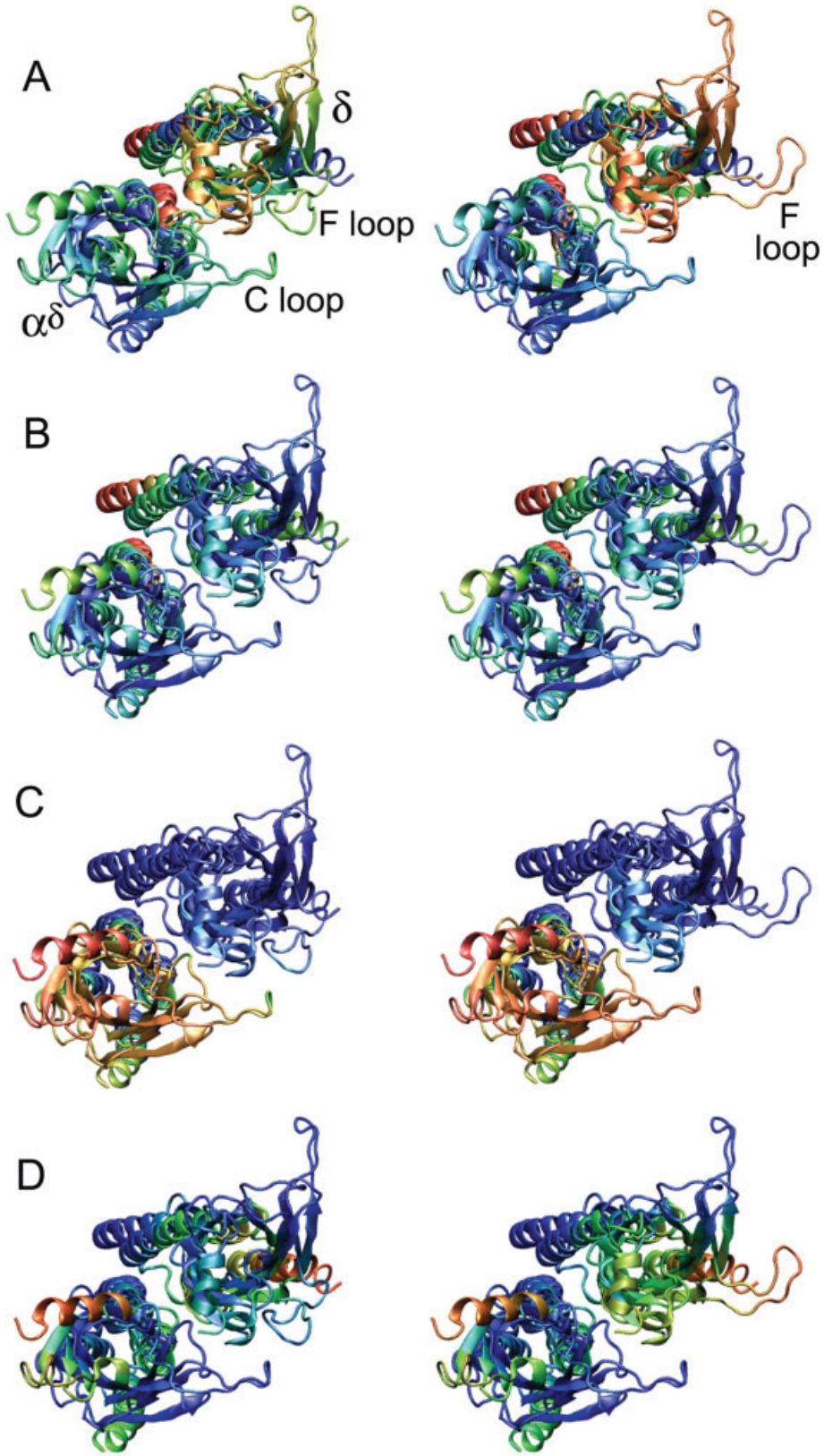

Figure 5

*Global and local dynamics are compared for types I–IV (**A–D**, respectively) between two energy-minimized F-loop conformations. Left column: F loop is tucked in the ligand binding site; Right column: F loop is extended out. Color codes for GNM fluctuations are the same as in Figures 2 and 3. The long F loop of the δ-subunit has a strong effect on the local fluctuation of the C-loop in the complementary α-subunits, but does not greatly change the global dynamics pattern of the receptor.*

helix and the loop linking TM1 and TM2 domains. A closer examination of the cross-correlation maps in Figure 4(A,B) reveals that other than the strong correlations among the five ICD helices, the only strong positive correlation that ICD helices have within the same subunit is with the TM1–2 loop. In addition, ICD helices also correlate with the TM1–2 loop of its adjacent subunits, but more so with the preceding than with the subsequent subunit [e.g., ICD of the β-subunit correlates more strongly with the TM1–2 loop of the α^{γ}-subunit than with TM1–2 loop of the δ-subunit, see Fig. 4(A)]. These correlations could by themselves be sufficient to modulate the pore behavior. It should be stressed that the ICD structure is incomplete in our calculations. Therefore, it is very plausible that this modulation is much stronger in the native receptors as the complete ICD loops are likely to interact more strongly with TMD.

In summary, we have shown the dynamical importance of the ICD, in line with the previous experimental findings. Clearly, the lack of structural information hinders computational work, especially on other Cys-loop receptors. It is, however, very clear from our study that due to the positive correlation between ICD and TMD, the ICD must be included in the calculation in order to account for its dynamical interplay with the pore domain.

Importance of the F loop

The structure, dynamics, and functional role of F loops have not been given much attention in previous computational studies. In the case of $(\alpha_7)_5$ nAChR modeled on the basis of the structure of acetylcholine binding protein, the F loop is relatively short. The non-α-subunits in *Torpedo* nAChR have significantly longer F loops and a poorer degree of sequence conservation among various subunits and receptor types. This fact alone could suggest that the F loops play an important role in ligand binding affinity and specificity, as suggested in several recent experiments showing differential F-loop involvement in the agonist versus antagonist binding in AChBP[74] and in the 5-HT_3 receptor,[75] and the nonequivalence of αγ and αδ ligand binding sites.[76–78]

In the currently available structure of *Torpedo* nAChR, all of the non-α-subunits, particularly the δ-subunit, have a long unresolved segment in their F loops. We have performed extensive conformational searches to select several possible low-energy conformers and investigated their impact on the local and global dynamics of the receptor. The missing fragments of the backbone are too long to be modeled with adequate accuracy, and the true (or "correct") conformations of these loops can only be ascertained when an experimental structure of these long loops becomes available. Therefore, rather than attempting to predict the structure, our aims were to investigate the flexibility of these fragments and the implications of this flexibility on the dynamics of the subunit interfaces. We have observed that the effects are most pronounced at the α^{δ}–δ interface, consistent with the fact that F loop in δ-subunit is the longest and so is its unresolved segment in the experimental structure, probably due to the intrinsically high flexibility.

Figure 5 compares the fluctuation distribution in the α^{δ}- and δ-subunits in two "extreme" F-loop conformations of the δ-subunit. Both conformations are energetically favorable. One of the conformations has the F loop "tucked" in the subunit body and in close contact with the C loop of the α^{δ}-subunit. The other conformation has the F loop swung away and extended. We have compared all motion types discussed above to evaluate the impact of the loop flexibility on the local and global scales. We found that such a drastic conformational difference had little effects on the global dynamics of the receptor. Correlation coefficients between all-receptor fluctuation distributions in the two conformers ranged from 87–99% (asymmetric types III and IV) to 96–100% (symmetric types I and II). There are no global changes in ANM motions, either. Thus, regardless of the F-loop conformation, the important types of global motion remain essentially the same. The detectable changes caused by the different F-loop conformations are confined locally in the adjacent subunits, predominantly in the LBDs. This is most pronounced in the α^{δ} C-loop, which is tightly coupled with the F loop of the δ-subunit. Depending on the conformation of the δ F loop, the flexibility of the C loop in α^{δ} can be increased or decreased. This regional dynamic interplay is very strong and has clear ligand-binding implications. The β-subunit, whose LBD is strongly correlated with that of the δ-subunit [Fig. 4(A)], is also affected by the local dependence on the F-loop conformation. In addition, there is a slight variation in the correlation between the F loop and TM2–3 loops, but the TM2 pore helices are not affected.

A possible concern about the GNM and ANM analyses of *Torpedo* nAChR with missing structural segments in F loops is the accuracy of loop modeling. The comparison of all-receptor correlation map shows that the changes are local and affect only the α^{δ}–δ interface. Hence, we can assume safely that the global patterns revealed by the GNM and ANM analyses are independent of the F-loop conformational details and the modeling inaccuracy.

In summary, we have shown that the F loops of the non-α-subunits, particularly the δ-subunit, play an important role in controlling the local dynamics of the binding interfaces. They are likely to affect the ligand binding affinity and specificity, but have little effects on global modes of channel motion.

CONCLUSIONS

Through GNM and ANM analyses, we have presented convincing data supporting the notion that a combina-

tion of symmetric and asymmetric motions contributes to gating in heteropentameric nAChR. Symmetric quaternary twist also exists in the heteropentameric receptor and is analogous to the twist motion reported for homopentamer neuronal receptor.[1,2] Because our model includes the intracellular helices, we have found that the twist motion exists in two different types depending on the dynamics at the TMD–ICD interface. Moreover, we have identified the asymmetric motion involving the tilting of the TM2 helices that is also likely to play a crucial role in gating.

In addition, our study reveals three additional features of the channel dynamics: (1) loop A, in addition to the CYS and β1–2 loops, serves as an allosteric mediator between the LBD and the loops at the LBD–TMD interface, particularly the TM2–3 loop; (2) ICD can modulate the pore dynamics and thus cannot be neglected in gating studies; and (3) the F loops, which are peculiarly longer and nonconserved in the non-α than in the α-subunits, have important dynamical impact locally at the ligand binding sites.

ACKNOWLEDGMENTS

The authors would like to thank Drs. Ivet Bahar and Indira Shrivastava for valuable comments. The research was facilitated by the allocation of advanced computing resources at the Pittsburgh Supercomputing Center through the support of the National Science Foundation and the Commonwealth of Pennsylvania.

REFERENCES

1. Cheng X, Lu B, Grant B, Law RJ, McCammon JA. Channel opening motion of alpha7 nicotinic acetylcholine receptor as suggested by normal mode analysis. J Mol Biol 2006;355:310–324.
2. Taly A, Delarue M, Grutter T, Nilges M, Le Novere N, Corringer PJ, Changeux JP. Normal mode analysis suggests a quaternary twist model for the nicotinic receptor gating mechanism. Biophys J 2005;88:3954–3965.
3. Sine SM, Engel AG. Recent advances in Cys-loop receptor structure and function. Nature 2006;440:448–455.
4. Karlin A. Emerging structure of the nicotinic acetylcholine receptors. Nat Rev Neurosci 2002;3:102–114.
5. Lester HA, Dibas MI, Dahan DS, Leite JF, Dougherty DA. Cys-loop receptors: new twists and turns. Trends Neurosci 2004;27:329–336.
6. Hansen SB, Radic Z, Talley TT, Molles BE, Deerinck T, Tsigelny I, Taylor P. Tryptophan fluorescence reveals conformational changes in the acetylcholine binding protein. J Biol Chem 2002;277:41299–41302.
7. Hansen SB, Radic Z, Talley TT, Taylor P Ligand binding characteristics of the acetylcholine binding proteins from *Lymnaea stagnalis* and *Aplysia californica*. Faseb J 2003, 17:A641–A641.
8. Hansen SB, Talley TT, Radic Z, Taylor P. Structural and ligand recognition characteristics of an acetylcholine-binding protein from *Aplysia californica*. J Biol Chem 2004;279:24197–24202.
9. Brejc K, van Dijk WJ, Klaassen RV, Schuurmans M, van Der Oost J, Smit AB, Sixma TK. Crystal structure of an ACh-binding protein reveals the ligand-binding domain of nicotinic receptors. Nature 2001;411:269–276.
10. Sixma TK, Smit AB. Acetylcholine binding protein (AChBP): a secreted glial protein that provides a high-resolution model for the extracellular domain of pentameric ligand-gated ion channels. Annu Rev Biophys Biomol Struct 2003;32:311–334.
11. Celie PH, van Rossum-Fikkert SE, van Dijk WJ, Brejc K, Smit AB, Sixma TK. Nicotine and carbamylcholine binding to nicotinic acetylcholine receptors as studied in AChBP crystal structures. Neuron 2004;41:907–914.
12. Celie PH, Kasheverov IE, Mordvintsev DY, Hogg RC, van Nierop P, van Elk R, van Rossum-Fikkert SE, Zhmak MN, Bertrand D, Tsetlin V, Sixma TK, Smit AB. Crystal structure of nicotinic acetylcholine receptor homolog AChBP in complex with an alpha-conotoxin PnIA variant. Nat Struct Mol Biol 2005;12:582–588.
13. Miyazawa A, Fujiyoshi Y, Unwin N. Structure and gating mechanism of the acetylcholine receptor pore. Nature 2003;423:949–955.
14. Unwin N. Refined structure of the nicotinic acetylcholine receptor at 4 Å resolution. J Mol Biol 2005;346:967–989.
15. Castillo M, Mulet J, Bernal JA, Criado M, Sala F, Sala S. Improved gating of a chimeric alpha7-5HT3A receptor upon mutations at the M2–M3 extracellular loop. FEBS Lett 2006;580:256–260.
16. Campos-Caro A, Sala S, Ballesta JJ, Vicente-Agullo F, Criado M, Sala F. A single residue in the M2–M3 loop is a major determinant of coupling between binding and gating in neuronal nicotinic receptors. Proc Natl Acad Sci USA 1996;93:6118–6123.
17. Rovira JC, Vicente-Agullo F, Campos-Caro A, Criado M, Sala F, Sala S, Ballesta JJ. Gating of alpha3beta4 neuronal nicotinic receptor can be controlled by the loop M2–M3 of both alpha3 and beta4 subunits. Pflugers Arch 1999;439:86–92.
18. Chakrapani S, Bailey TD, Auerbach A. The role of loop 5 in acetylcholine receptor channel gating. J Gen Physiol 2003;122:521–539.
19. Chakrapani S, Bailey TD, Auerbach A. Gating dynamics of the acetylcholine receptor extracellular domain. J Gen Physiol 2004;123:341–356.
20. Lee WY, Sine SM. Principal pathway coupling agonist binding to channel gating in nicotinic receptors. Nature 2005;438:243–247.
21. Lummis SC, Beene DL, Lee LW, Lester HA, Broadhurst RW, Dougherty DA. Cis–trans isomerization at a proline opens the pore of a neurotransmitter-gated ion channel. Nature 2005;438:248–252.
22. Xiu X, Hanek AP, Wang J, Lester HA, Dougherty DA. A unified view of the role of electrostatic interactions in modulating the gating of cys loop receptors. J Biol Chem 2005;280:41655–41666.
23. Grosman C, Zhou M, Auerbach A. Mapping the conformational wave of acetylcholine receptor channel gating. Nature 2000;403:773–776.
24. Unwin N, Miyazawa A, Li J, Fujiyoshi Y. Activation of the nicotinic acetylcholine receptor involves a switch in conformation of the alpha subunits. J Mol Biol 2002;319:1165–1176.
25. Grosman C, Auerbach A. Asymmetric and independent contribution of the second transmembrane segment 12′ residues to diliganded gating of acetylcholine receptor channels: a single-channel study with choline as the agonist. J Gen Physiol 2000;115:637–651.
26. Dahan DS, Dibas MI, Petersson EJ, Auyeung VC, Chanda B, Bezanilla F, Dougherty DA, Lester HA. A fluorophore attached to nicotinic acetylcholine receptor beta M2 detects productive binding of agonist to the alpha delta site. Proc Natl Acad Sci USA 2004;101:10195–10200.
27. Grandl J, Danelon C, Hovius R, Vogel H. Functional asymmetry of transmembrane segments in nicotinic acetylcholine receptors. Eur Biophys J 2006;35:685–693.
28. Wilson G, Karlin A. Acetylcholine receptor channel structure in the resting, open, and desensitized states probed with the substituted-cysteine-accessibility method. Proc Natl Acad Sci USA 2001;98:1241–1248.
29. Wilson GG, Karlin A. The location of the gate in the acetylcholine receptor channel. Neuron 1998;20:1269–1281.

 DOI 10.1002/prot

30. Beckstein O, Sansom MS. A hydrophobic gate in an ion channel: the closed state of the nicotinic acetylcholine receptor. Phys Biol 2006;3:147–159.
31. Saladino AC, Xu Y, Tang P. Homology modeling and molecular dynamics simulations of transmembrane domain structure of human neuronal nicotinic acetylcholine receptor. Biophys J 2005;88:1009–1017.
32. Saiz L, Klein ML. The transmembrane domain of the acetylcholine receptor: insights from simulations on synthetic peptide models. Biophys J 2005;88:959–970.
33. Hung A, Tai K, Sansom MS. Molecular dynamics simulation of the M2 helices within the nicotinic acetylcholine receptor transmembrane domain: structure and collective motions. Biophys J 2005;88: 3321–3333.
34. Xu Y, Barrantes FJ, Luo X, Chen K, Shen J, Jiang H. Conformational dynamics of the nicotinic acetylcholine receptor channel: a 35-ns molecular dynamics simulation study. J Am Chem Soc 2005;127:1291–1299.
35. Law RJ, Henchman RH, McCammon JA. Chemical theory and computation special feature: A gating mechanism proposed from a simulation of a human alpha7 nicotinic acetylcholine receptor. Proc Natl Acad Sci USA 2005;102:6813–6818.
36. Adcock C, Smith GR, Sansom MS. The nicotinic acetylcholine receptor: from molecular model to single-channel conductance. Eur Biophys J 2000;29:29–37.
37. Sansom MS, Adcock C, Smith GR. Modelling and simulation of ion channels: applications to the nicotinic acetylcholine receptor. J Struct Biol 1998;121:246–262.
38. Amiri S, Tai K, Beckstein O, Biggin PC, Sansom MSP. The alpha 7 nicotinic acetylcholine receptor: molecular modelling, electrostatics, and energetics. Mol Membr Biol 2005;22:151–162.
39. Henchman RH, Wang HL, Sine SM, Taylor P, McCammon JA. Asymmetric structural motions of the homomeric alpha7 nicotinic receptor ligand binding domain revealed by molecular dynamics simulation. Biophys J 2003;85:3007–3018.
40. Shrivastava IH, Bahar I. Common mechanism of pore opening shared by five different potassium channels. Biophys J 2006;90: 3929–3940.
41. Arias HR, Bhumireddy P, Spitzmaul G, Trudell JR, Bouzat C. Molecular mechanisms and binding site location for the noncompetitive antagonist crystal violet on nicotinic acetylcholine receptors. Biochemistry 2006;45:2014–2026.
42. Bouzat C, Bren N, Sine SM. Structural basis of the different gating kinetics of fetal and adult acetylcholine receptors. Neuron 1994;13: 1395–1402.
43. Wang HL, Ohno K, Milone M, Brengman JM, Evoli A, Batocchi AP, Middleton LT, Christodoulou K, Engel AG, Sine SM. Fundamental gating mechanism of nicotinic receptor channel revealed by mutation causing a congenital myasthenic syndrome. J Gen Physiol 2000;116:449–462.
44. Kelley SP, Dunlop JI, Kirkness EF, Lambert JJ, Peters JA. A cytoplasmic region determines single-channel conductance in 5-HT3 receptors. Nature 2003;424:321–324.
45. Hu XQ, Sun H, Peoples RW, Hong R, Zhang L. An interaction involving an arginine residue in the cytoplasmic domain of the 5-HT3A receptor contributes to receptor desensitization mechanism. J Biol Chem 2006;281:21781–21788.
46. Atilgan AR, Durell SR, Jernigan RL, Demirel MC, Keskin O, Bahar I. Anisotropy of fluctuation dynamics of proteins with an elastic network model. Biophys J 2001;80:505–515.
47. Bahar I, Erman B, Haliloglu T, Jernigan RL. Efficient characterization of collective motions and interresidue correlations in proteins by low-resolution simulations. Biochemistry 1997;36:13512–13523.
48. Xu C, Tobi D, Bahar I. Allosteric changes in protein structure computed by a simple mechanical model: hemoglobin TR2 transition. J Mol Biol 2003;333:153–168.
49. Yang LW, Bahar I. Coupling between catalytic site and collective dynamics: a requirement for mechanochemical activity of enzymes. Structure (Camb) 2005;13:893–904.
50. Ma J. Usefulness and limitations of normal mode analysis in modeling dynamics of biomolecular complexes. Structure 2005;13:373–380.
51. Ma JP. New advances in normal mode analysis of supermolecular complexes and applications to structural refinement. Curr Protein Pept Sc 2004;5:119–123.
52. Tozzini V. Coarse-grained models for proteins. Curr Opin Struct Biol 2005;15:144–150.
53. Tama F. Normal mode analysis with simplified models to investigate the global dynamics of biological systems. Protein Pept Lett 2003;10: 119–132.
54. Doruker P, Atilgan AR, Bahar I. Dynamics of proteins predicted by molecular dynamics simulations and analytical approaches: application to alpha-amylase inhibitor. Proteins 2000;40:512–524.
55. Bahar I, Atilgan AR, Erman B. Direct evaluation of thermal fluctuations in proteins using a single-parameter harmonic potential. Fold Des 1997;2:173–181.
56. Haliloglu T, Bahar I, Erman B. Gaussian dynamics of folded proteins. Phys Rev Lett 1997;79:3090–3093.
57. Tama F, Sanejouand YH. Conformational change of proteins arising from normal mode calculations. Protein Eng 2001;14:1–6.
58. Ma J. Usefulness and limitations of normal mode analysis in modeling dynamics of biomolecular complexes. Structure (Camb) 2005;13: 373–380.
59. Yang LW, Liu X, Jursa CJ, Holliman M, Rader AJ, Karimi HA, Bahar I. iGNM: a database of protein functional motions based on Gaussian Network Model. Bioinformatics 2005;21:2978–2987.
60. Suhre K, Sanejouand YH. ElNemo: a normal mode web server for protein movement analysis and the generation of templates for molecular replacement. Nucleic Acids Res 2004;32(Web Server issue): W610–W614.
61. Tama F, Gadea FX, Marques O, Sanejouand YH. Building-block approach for determining low-frequency normal modes of macromolecules. Proteins 2000;41:1–7.
62. Delarue M, Sanejouand YH. Simplified normal mode analysis of conformational transitions in DNA-dependent polymerases: the elastic network model. J Mol Biol 2002;320:1011–1024.
63. Phillips JC, Braun R, Wang W, Gumbart J, Tajkhorshid E, Villa E, Chipot C, Skeel RD, Kale L, Schulten K. Scalable molecular dynamics with NAMD. J Comput Chem 2005;26:1781–1802.
64. Smart OS, Neduvelil JG, Wang X, Wallace BA, Sansom MS. HOLE: a program for the analysis of the pore dimensions of ion channel structural models. J Mol Graph 1996;14:354–360, 376.
65. Humphrey W, Dalke A, Schulten K. VMD: visual molecular dynamics. J Mol Graph 1996;14:33–38, 27–38.
66. Fiser A, Do RK, Sali A. Modeling of loops in protein structures. Protein Sci 2000;9:1753–1773.
67. Fiser A, Sali A. ModLoop: automated modeling of loops in protein structures. Bioinformatics 2003;19:2500–2501.
68. Laskowski RA, Macarthur MW, Moss DS, Thornton JM. Procheck—a program to check the stereochemical quality of protein structures. J Appl Crystallogr 1993;26:283–291.
69. Jensen ML, Schousboe A, Ahring PK. Charge selectivity of the Cys-loop family of ligand-gated ion channels. J Neurochem 2005;92: 217–225.
70. Beckstein O, Sansom MS. The influence of geometry, surface character, and flexibility on the permeation of ions and water through biological pores. Phys Biol 2004, 1:42–52.
71. Auerbach A, Akk G. Desensitization of mouse nicotinic acetylcholine receptor channels. A two-gate mechanism. J Gen Physiol 1998;112:181–197.
72. Hansen SB, Sulzenbacher G, Huxford T, Marchot P, Taylor P, Bourne Y. Structures of aplysia AChBP complexes with nicotinic agonists and antagonists reveal distinctive binding interfaces and conformations. Embo J 2005;24:3635–3646.

73. Chanda B, Asamoah OK, Blunck R, Roux B, Bezanilla F. Gating charge displacement in voltage-gated ion channels involves limited transmembrane movement. Nature 2005;436:852–856.
74. Shi J, Koeppe JR, Komives EA, Taylor P. Ligand-induced conformational changes in the acetylcholine-binding protein analyzed by hydrogen–deuterium exchange mass spectrometry. J Biol Chem 2006;281:12170–12177.
75. Thompson AJ, Padgett CL, Lummis SC. Mutagenesis and molecular modeling reveal the importance of the 5-HT3 receptor F-loop. J Biol Chem 2006;281:16576–16582.
76. Andreeva IE, Nirthanan S, Cohen JB, Pedersen SE. Site specificity of agonist-induced opening and desensitization of the Torpedo California nicotinic acetylcholine receptor. Biochemistry 2006;45:195–204.
77. Blount P, Merlie JP. Molecular basis of the two nonequivalent ligand binding sites of the muscle nicotinic acetylcholine receptor. Neuron 1989;3:349–357.
78. Prince RJ, Sine SM. Molecular dissection of subunit interfaces in the acetylcholine receptor. Identification of residues that determine agonist selectivity. J Biol Chem 1996;271:25770–25777.

 DOI 10.1002/prot